

Optimizing the Dynamic Response of Microsatellite Yaw-axis Attitude Using LQR-Based Control System

Emmanuel E. Egwim¹; Ikemsinachi Chikeziri Osuagwu²; Cyprian Izuchukwu Igwedibia³; Lawrence Chukwuebuka Onyebuchukwu⁴

¹Department of Electrical and Electronic Engineering Bells University of Technology Ota, Nigeria

²Department of Electronic Engineering Federal University of Technology Owerri Owerri, Nigeria

^{3,4}Department of Electrical and Electronic Engineering Imo State University Owerri, Nigeria

Publication Date: 2026/06/23

Abstract

The importance of effective satellite attitude control system is that it can ensure both quality and reliability of data acquisition by a microsatellite. In this paper, an optimal controller is designed for microsatellite yaw-axis attitude control system. In order to achieve this, the dynamic models of microsatellite yaw-axis attitude are obtained. Then an optimal controller based on Linear Quadratic Regulator (LQR) is designed. The designed LQR is integrated into the closed loop network of the microsatellite yaw-axis attitude control system. A MATLAB/Simulink model, which is computer-based model, is developed using the mathematical models of the closed control system. The MATLAB/Simulink model was used to conduct computer simulation of microsatellite attitude with the LQR. The simulation analysis revealed that the proposed LQR improve the transient and steady-state performance of the system in terms of rise time, settling time, overshoot, and steady-state error.

Keywords: Attitude Control System, LQR, Microsatellite, Optimal Controller, Yaw-Axis.

I. INTRODUCTION

Despite the fact that PID controllers are largely employed in many industrial process control operations because of the associated simple structure and function including ease of design, their performance are largely affected by mismatch or variation in system parameters [1]. Also, PID controller is considered a linear control system and has poor anti-interference ability, and with the disadvantage of depending on manual adjustment of its parameter [2]. Therefore, several other control techniques that have been implemented to address the shortcoming of the classical control methods. For instance, Linear Quadratic tracker (LQT) with the combination of integral compensator or Exponential Control Mapping (ECM) has been used to evaluate the performance of satellite ACS techniques with 4 Control Moment Gyroscopes (CMGs) configured in pyramidal pattern [3]. Software-in-the-loop (SIL) techniques has been used in the development of a microsatellite attitude determination and control system (ADCS) that

implements thrusters in plus-wide modulation control technique to reduce the angular velocity of satellite [4]. The performance of fuzzy logic control algorithm, classical PID control scheme and modified PID control scheme was experimentally compared on a laboratory nanosatellite and its testing system to draw ascertain their effectiveness with respect to robustness, accuracy (based on steady state error), convergence time, and energy conservation with results obtained indicating that fuzzy controller outperformed the PID [5]. A control system based on maximum principle of Pontryagin together with a full order estimator using linear state variable feedback was used in ACS of a space satellite [6]. A satellite attitude in three operating modes namely, detumbling after isolation from the launcher, nominal operation when the satellite attitude is subjected to slight or moderate perturbation, and momentum unloading following reaction wheel saturation, has been controlled using a generic model of nanosatellite with PID controllers with selectable gains [7]. Attitude control of under-actuated spacecraft that uses solar radiation

pressure has been achieved using integrated control technique based on dual-model predictive control [8]. The convergence rate and robustness of satellite attitude control system was achieved using a variable structure PID control technique [9]. Quick transient response and zero steady-state error for satellite ACS was achieved using a PID controller [10]. A three-axis attitude digital controller based on Linear Quadratic Gaussian (LQG) regulator method that was developed using digital signal processor has been used for satellite attitude control [11]. Performance comparison of PID controller and LQR control method in Low Earth Orbit (LEO) satellite attitude stabilization was conducted such that simulation result revealed PID algorithm was unable to stabilize the system after 500 s [12]. Control technique based on the Lyapunov stability control theory was used to achieve attitude reference trajectory [13]. Direct Torque Control

(DTC) method that was designed using PID controller plus DTC on actuator was applied for stabilizing roll, pitch and yaw angles of satellite [14]. PID controller was used for nanosatellite to provide in improve transient response of attitude control system [15]. As spacecraft attitude control actuators control moment gyroscope (CMG) is considered suitable for three axes manoeuvring such as roll, pitch and yaw-axis and was implemented for three-axis attitude control for agile satellites [16]. The dynamic characteristics of a microsatellite have been enhanced using reference model based PID and discrete-time PID in [17] and [18], respectively.

The structure of a microsatellite with reference body coordinate frames in terms of pitch, roll and yaw-axis is shown in Fig. 1.

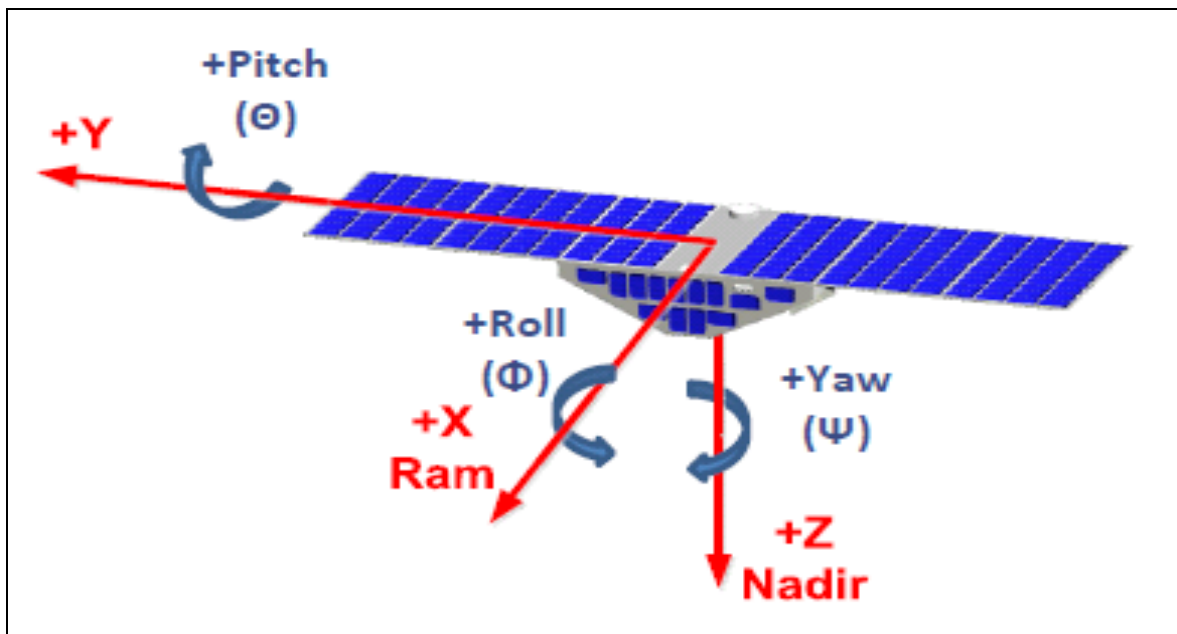


Fig 1 Structure of Microsatellite System with Reference Coordinate Frames [19]

In this paper, an optimal control based on Linear Quadratic Regulator (LQR) technique is proposed for microsatellite yaw-axis ACS to improve tracking and stability performance is proposed. This way, the system will be able to maintain reliable adjustment and stability during its flight operation. The primary goal of is to achieve fast convergence and improved overshoot around reference attitude.

II. SYSTEM DESIGN AND SPECIFICATIONS

➤ System Description

The block diagram description of microsatellite yaw-axis ACS is shown in Fig. 2 with its subsystem dynamics presented as transfer functions for the amplifier $G_{amp}(s)$, actuator $G_a(s)$ and the satellite structure $G_{sat}(s)$ as defined by (1) to (3).

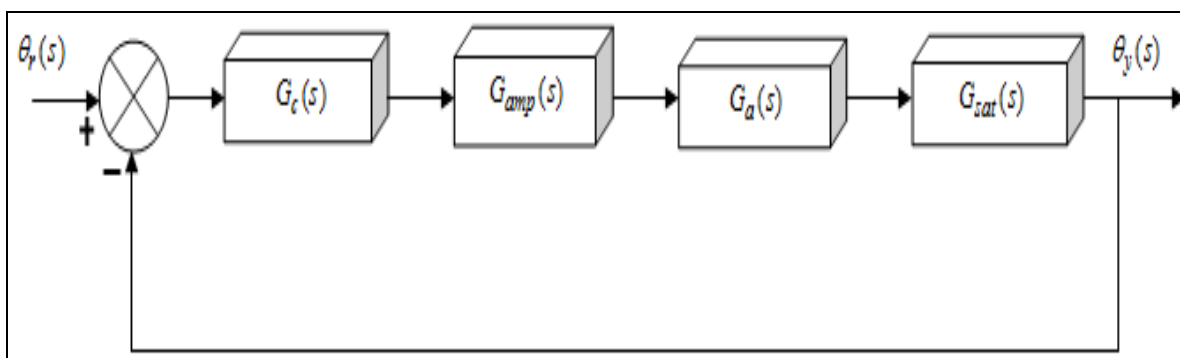


Fig 2 Microsatellite Yaw-Axis ACS Block Diagram

Hence, from the block diagram the following parameters are defined [20]:

$$G_{sat}(s) = \frac{1}{0.8s^2} \quad (1)$$

$$G_a(s) = \frac{78.3s}{s^2 + 1815.4s + 24466} \quad (2)$$

$$G_{amp}(s) = \frac{240}{0.1s + 1} \quad (3)$$

In Fig. 1, $G_c(s)$ represents the transfer function for PID controller as [20], which will be replaced with a LQR in this paper. Thus, the closed loop transfer function of the system without the PID controller is given by:

$$\frac{\theta_y(s)}{\theta_r(s)} = \frac{18792s}{0.08s^5 + 146s^4 + 3410s^3 + 1.957e04s^2} \quad (4)$$

The system will hence forth be evaluated in state space form rather than transfer function. This is because to design LQR, the system has to be represented in state space form.

➤ State Space Modelling

The state space modelling of microsatellite yaw-axis ACS is described in this subsection section. State space model is a mathematical expression that is used to relate the input variable(s), the state variables and the output variables of a system. This is achieved by carrying out the mathematical modelling of a system which, together with the output, provides information regarding the state of the system variables at a certain fixed points along the flow of signals [21]. State variable design provides the basis for modern control theory and system optimization and it is directly a time domain technique [21,22]. In addition, it is considered an influential technique for analysis and design of linear, nonlinear, and time invariant or time varying multiple input multiple output

system [3]. The general form to represent a linear time invariant single input single output system in state space form [21, 23] is given by:

$$\dot{x} = Ax + Bu \quad (5)$$

$$y = Cx + Du \quad (6)$$

Where A is the state matrix, B is the input matrix, C is the output matrix, and D is the direct transition matrix (which is zero in this case). Hence, using the MATLAB syntax (`>>sys = ss (G)`) transforms the closed loop transfer function in (4) to state space equation given by:

$$\begin{bmatrix} \dot{x}_1 \\ \dot{x}_2 \\ \dot{x}_3 \\ \dot{x}_4 \\ \dot{x}_5 \end{bmatrix} = \begin{bmatrix} -1825 & -166.5 & -29.87 & 0 & 0 \\ 256 & 0 & 0 & 0 & 0 \\ 0 & 32 & 0 & 0 & 0 \\ 0 & 0 & 0.25 & 0 & 0 \\ 0 & 0 & 0 & 0.25 & 0 \end{bmatrix} \begin{bmatrix} x_1 \\ x_2 \\ x_3 \\ x_4 \\ x_5 \end{bmatrix} + \begin{bmatrix} 8 \\ 0 \\ 0 \\ 0 \\ 0 \end{bmatrix} u(t) \quad (7)$$

$$y = [0 \ 0 \ 0 \ 14.34 \ 0] [x_1 \ x_2 \ x_3 \ x_4 \ x_5]^T \quad (8)$$

Where,

$$A = \begin{bmatrix} -1825 & -166.5 & -29.87 & 0 & 0 \\ 256 & 0 & 0 & 0 & 0 \\ 0 & 32 & 0 & 0 & 0 \\ 0 & 0 & 0.25 & 0 & 0 \\ 0 & 0 & 0 & 0.25 & 0 \end{bmatrix}, B = \begin{bmatrix} 8 \\ 0 \\ 0 \\ 0 \\ 0 \end{bmatrix}, C = [0 \ 0 \ 0 \ 14.34 \ 0], D = 0.$$

Equations (7) and (8) conform to (5) and (6).

➤ Design Specifications

The design specifications of the system given unit step input are presented in Table 1. The system peak overshoot (PO) is taken as a measure of the damping, while the settling time (t_s) is the time for the response of the system to remain within 2% of the final value.

Table 1 Performance Specifications [20]

Parameters	Values
Percentage overshoot (PO)	$\leq 5\%$
Settling time (t_s) for 2% criterion	$\leq 2 \text{ s}$
Steady state error	0

➤ Design of LQR Control System

The proposed microsatellite yaw-axis ACS using LQR algorithm is presented in this section. The LQR technique is employed in modern optimal control theory and has been extensively used besides PID controller in many control applications due to its stability [24]. The main aim of LQR as an optimal state feedback controller is to minimize the quadratic cost function given by [25]:

$$J = \frac{1}{2} \int_0^{\infty} [x^T(t)Qx(t) + u^T(t)Ru(t)] dt \quad (9)$$

Where $R = R^T > 0$ and $Q = Q^T > 0$ are weighting factor of control variables and state variables, which are positive definite matrix and positive semi-definite matrix respectively. Equation (9) ensures that the controller provides optimal response. In order to achieve this, the

design of LQR is carried out considering three steps. However, to start the design of LQR, the following is assumed: the model of the plant is perfectly known and all states are directly measurable (i.e. available for feedback) [24].

The first step involves selecting the state and control law matrices, Q and R respectively. The control law guarantees that the output is maintained as close as possible to the desire value with minimum cost. Generally, Q is varied while R fixed during the design, which is performed based on the performance specifications defined the designer.

In step two, the algebraic Riccati equation is solved. In order to determine the optimal gain matrix K of the

control law, the designer first obtains the Riccati coefficient matrix P , which is the unique, symmetric matrix of the Riccati equation given by [26]:

$$PA + A^T P - PBR^{-1}B^T P + Q = 0 \quad (10)$$

The values for Q, R, P were obtained in this paper using appropriate MATLAB syntax. Hence the following were obtained:

$$Q = \begin{bmatrix} 100000 & 0 & 0 & 0 & 0 \\ 0 & 0.001 & 0 & 0 & 0 \\ 0 & 0 & 0.001 & 0 & 0 \\ 0 & 0 & 0 & 10000 & 0 \\ 0 & 0 & 0 & 0 & 0.001 \end{bmatrix}, R = [1],$$

$$P = \begin{bmatrix} 20.3 & 1.3 & 0.5 & 12.5 & 0 \\ 1.3 & 29.6 & 8.8 & 152.7 & 0 \\ 0.5 & 8.8 & 4.2 & 98.7 & 0 \\ 12.5 & 152.7 & 98.7 & 3181.7 & 1 \\ 0 & 0 & 0 & 1 & 12.6 \end{bmatrix}$$

The third step involves obtaining the optimal control law gain matrix K . Therefore, given a system $\dot{x} = Ax + Bu$ with a non-zero initial state $x(0)$, the input $u(t)$ is determined by minimizing the cost function. The input takes the system to zero state in optimal manner

and it is regarded as the feedback control law of the optimal controller (LQR) that minimizes the cost function. It is given by:

$$u = -Kx \quad (11)$$

Where,

$$K = R^{-1}B^T P \quad (12)$$

The values of K can be obtained using appropriate MATLAB syntax based on (12) or using the MATLAB syntax $K = lqr(A, B, Q, R)$. The obtained gain matrix from the software computation is:

$$K = [162.6811 \quad 10.7561 \quad 4.2204 \quad 100.0025 \quad 0.0316] \quad (13)$$

Hence, the designed optimal control law substituting (13) into (11) is given by:

$$u = [162.6811 \quad 10.7561 \quad 4.2204 \quad 100.0025 \quad 0.0316]x \quad (14)$$

The Simulink model of the proposed LQR based microsatellite yaw-axis ACS is shown in Figure 3. The Simulink diagram for the comparison of the proposed system and various PID-based control techniques implemented in previous study by [20] is shown in Fig. 4.

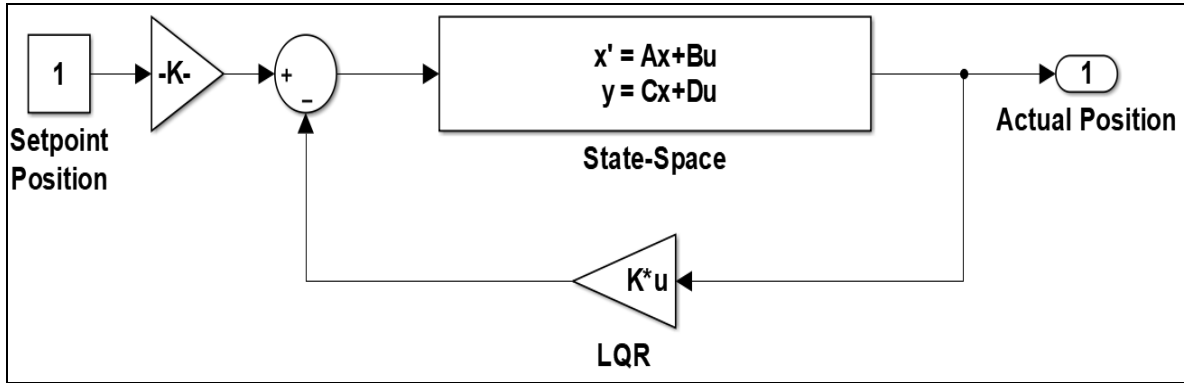


Fig 3 LQR Based Microsatellite Yaw-Axis ACS

The mathematical models of ITAE based PID controlled system without pre-filter (PID), PID controlled system with pre-filter (PIDf), PD controlled system

without pre-filter, and PD controlled system with pre-filter (PID) as in [20] are given by:

$$G_{hcclpid} = \frac{189200(s + 11.34)(s + 3.3630)}{s^5 + 1825s^4 + 42625s^3 + 43380s^2 + 2783000s + 7219000} \quad (15)$$

$$G_{hcclpidf} = \left(\frac{38.16}{s^2 + 14.71s + 38.16} \right) \times \left(\frac{189200(s + 11.34)(s + 3.3630)}{s^5 + 1825s^4 + 42625s^3 + 43380s^2 + 2783000s + 7219000} \right) \quad (16)$$

$$G_{hcclpd} = \frac{98870(s+13.07)}{s^4 + 1825s^3 + 42625s^2 + 343500s + 1292000} \quad (17)$$

$$G_{hcclpdf} = \left(\frac{13.07}{s+13.07} \right) \left(\frac{98870(s+13.07)}{s^4 + 1825s^3 + 42625s^2 + 343500s + 1292000} \right) \quad (18)$$

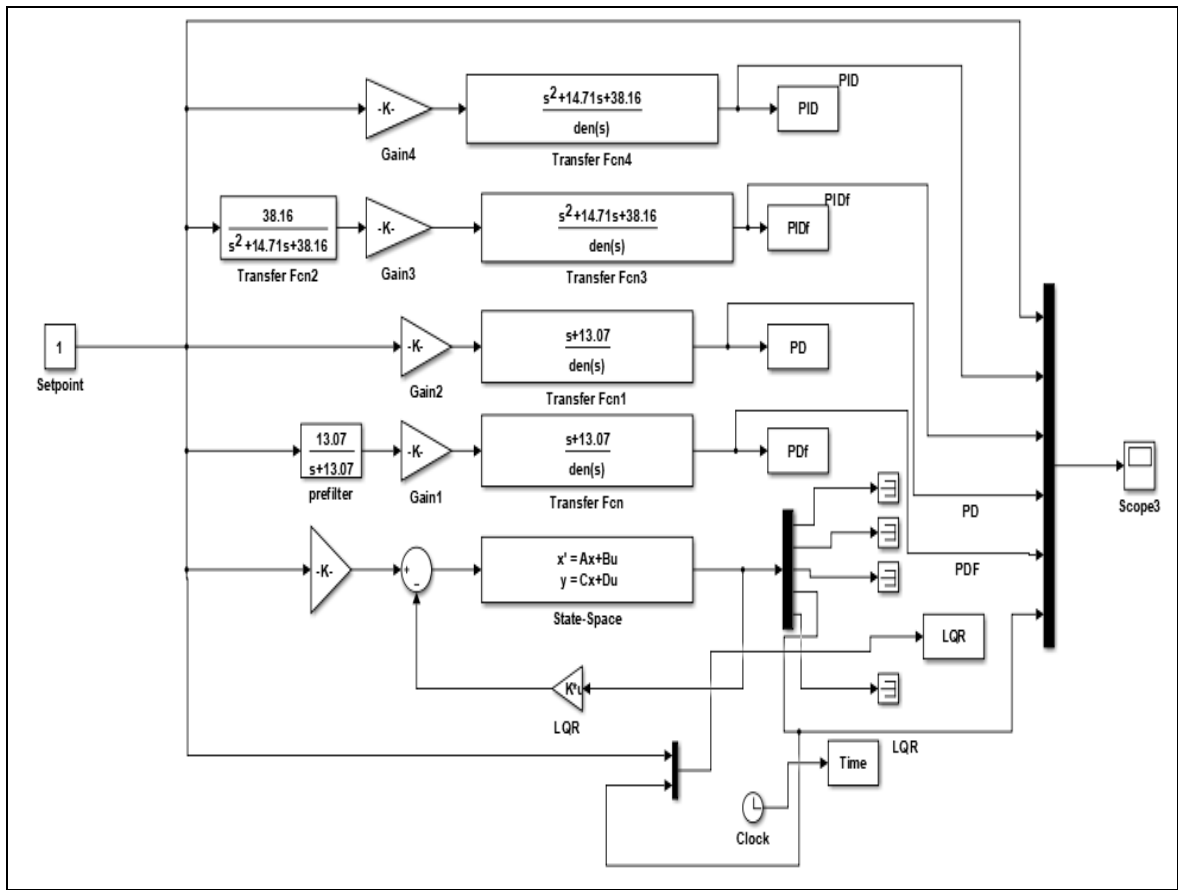


Fig 4 Simulink Block Diagram for Comparison of LQR and Classical PID Techniques

III. RESULTS AND DISCUSSION

In order to analyse the transient and steady state characteristics of the proposed system, simulations were conducted basically for three different scenarios to justify and validate significance of the study. Simulation based on unit step input was initially conducted for closed loop response of the microsatellite yaw-axis ACS without incorporating any controller in the loop to compensate for system performance as shown in Fig. 5. This regarded as uncontrolled or uncompensated system. In the next

approach, the designed LQR was considered as part of the closed loop and simulation was performed for unit step input as shown in Figure 6. Lastly, simulation for performance comparison was carried out with LQR and previous schemes based on PID and its versions implemented in the study carried out by [2] for the same microsatellite yaw-axis ACS as shown in Figure 7. The numerical analysis of the system the various step responses obtained from the simulations conducted are summarized in Table 2.

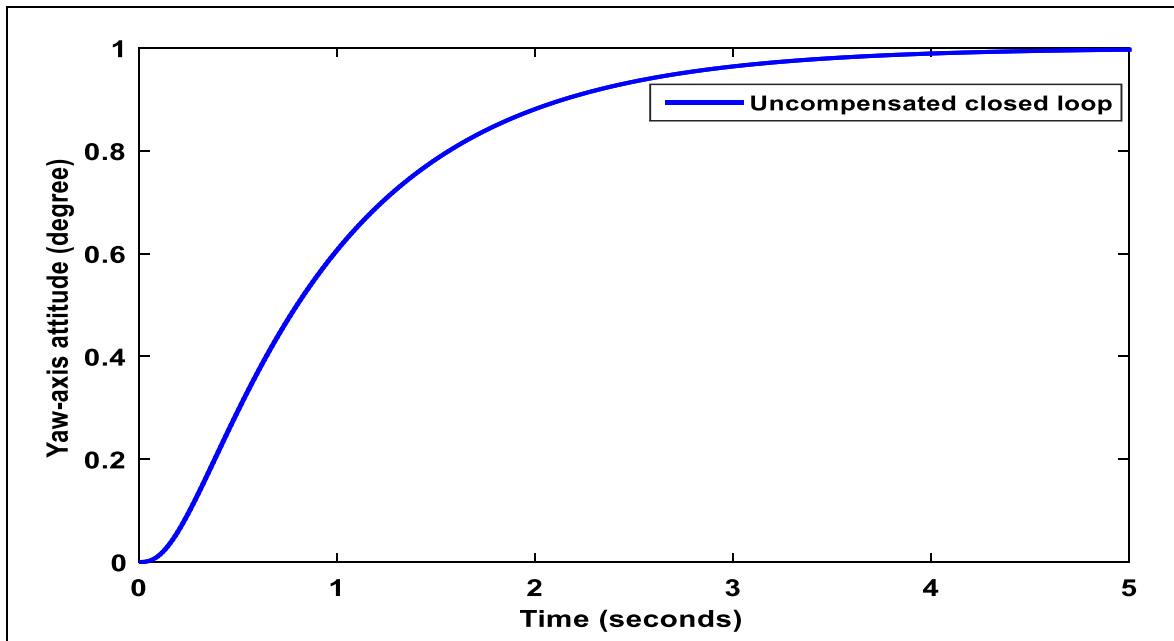


Fig 5 Step Response for Uncompensated System

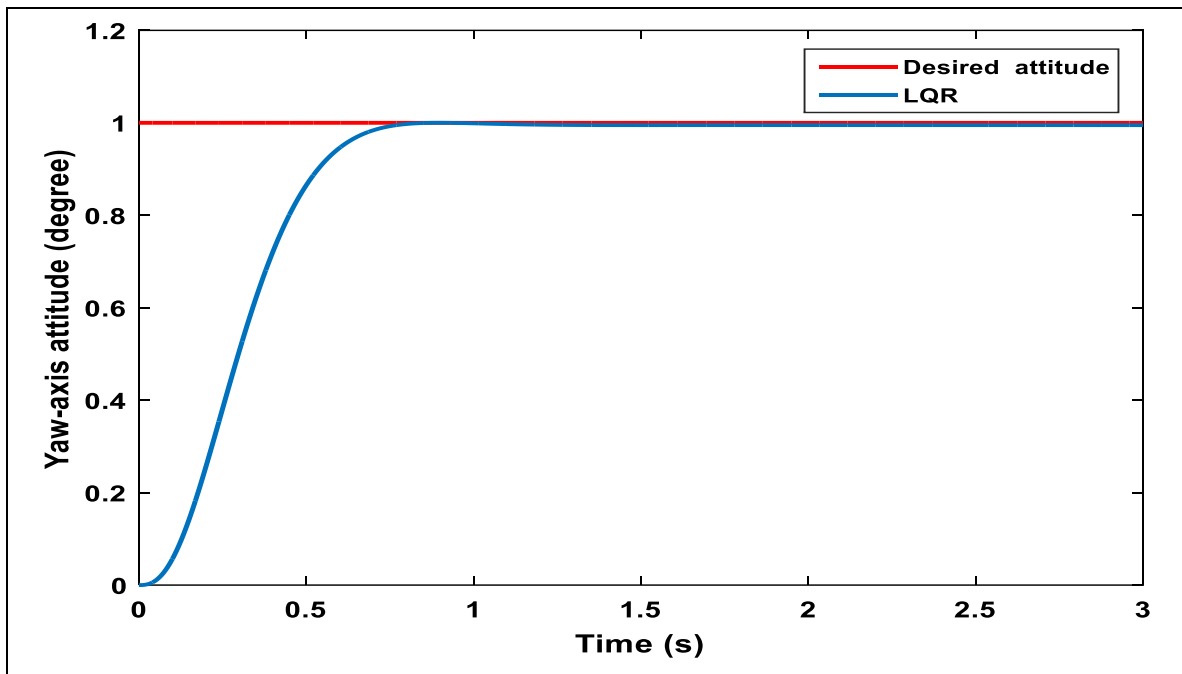


Fig 6 Step Response for LQR Controlled System

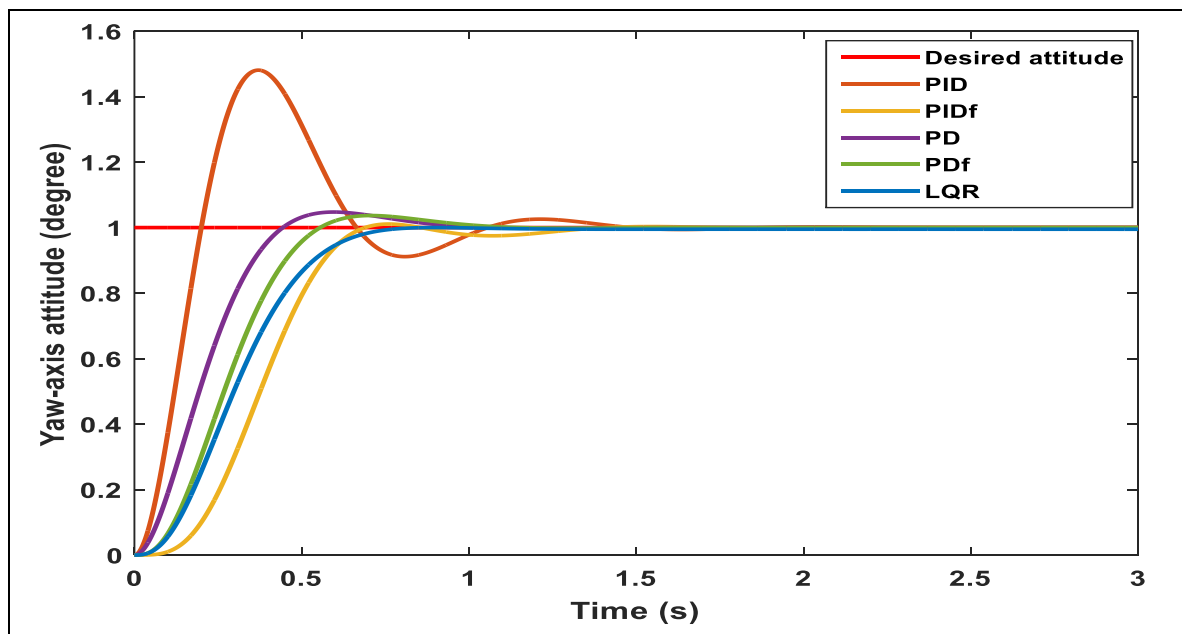


Fig 7 Step Responses for Performance Comparison

Table 2 Numerical Analysis of System Performance

System condition	t_r (s)	t_s (s)	PO (%)	t_p (s)	Ess
Un-comp. system	1.865	3.366	0	5	0
PID	0.135	1.305	48.05	0.370	0
PIDf	0.365	1.175	1.075	0.760	0
PD	0.287	0.814	4.726	0.595	0
PDf	0.332	0.887	3.663	0.707	0
LQR	0.403	0.668	0.508	0.897	0

Note regarding Figure 6 and Table 2: PIDf means Proportional Integral and Derivative (PID) with pre-filter, PD means Proportional Derivative (PD), and PDf means Proportional Derivative (PD) with pre-filter, t_r is the rise time, t_s is the settling time, PO is the peak overshoot, t_p is the peak time, and E_{ss} is the steady-state error.

The explanation of the performance of the system is better understood considering the design specifications provided in subsection 2.2. It can be seen from the simulation analysis looking at Table 2 that the only condition of the system when the performance specifications were not met was the uncompensated state. Thus, the need for sub-unit that will act as a controller to

compensate for the weakness associated with the uncontrolled microsatellite yaw-axis ACS. The addition of the various control algorithm shows that design specifications were achieved in almost all the cases except for the PID system that resulted in peak overshoot of 48.0477%. Hence, of the five scenarios with controller to compensate for system performance and to met design specifications only four satisfy the system design requirement defined as settling time less than or equal to 2 s ($t_s \leq 2$ s), peak overshoot less than or equal to 5% ($PO \leq 5\%$), and $E_{ss} = 0$. These are PID with pre-filter (PIDf) control system, PD control system, PD with pre-filter (PDf) control system, and LQR control system. From the numerical analysis considering the design specifications, the LQR offers the best performance with settling time of 0.6676 s and overshoot of 0.5083%. It suffices to say that the proposed LQR system will provide the best stable and reliable performance compare with the other controllers.

IV. CONCLUSION

An optimal controller based on LQR has been designed as a sub-unit for microsatellite yaw-axis ACS. The dynamic characteristics of microsatellite yaw-axis ACS was established as transfer functions for amplifier circuit, actuator device, and satellite structure respectively. These transfer functions were combined and implemented with unity feedback network to give the closed loop dynamic behaviour of the system as transfer function, which is a complex frequency domain (s-domain) representation. The resulted closed loop transfer function model was transformed into equivalent state space dynamic characteristics, which is a time-domain representation. Then a LQR was designed and integrated into the system to compensate for its performance. The results from the simulation indicated the LQR improves the system performance in terms of rise time, settling time, overshoot, and steady-state error; and outperformed other control structure based on PID, PIDf, PD, and PIDf controllers.

REFERENCES

- [1]. Agwah, B. C., & Eze, P. C. (2022). An intelligent controller augmented with variable zero lag compensation for antilock braking system. *International Journal of Mechanical and Mechatronics Engineering*, 16(11), 303-310.
- [2]. Shan, Y., Xia, L., & Li, S. (2022). Design and simulation of satellite attitude control algorithm based on PID. *Journal of Physics: Conference Series*, 2355 012035. <https://doi.org/10.1088/1742-6596/2355/1/012035>
- [3]. Portella, K. M., Schinestzki, W. N., Sehnem, R. M., da Luz, L. B., Mantovani, L. Q., Sacco, R. R., Kraemer, S. S., & Paglione, P. (2020). Satellite attitude control using control moment gyroscopes. *Journal of Aerospace Technology and Management, São José dos Campos*, 12, 94-105. <https://doi.org/10.5028/jatm.cab.1156>
- [4]. Shou, H.-N. (2014). Microsatellite attitude determination and control subsystem design and implementation: software-in-the-loop approach. *Mathematic Problems in Engineering, Volume 2014*, Article ID 904708, 1-13. <http://dx.doi.org/10.1155/2014/904708>
- [5]. Bello, A., Olfe, K. S., Rodríguez, J. Ezquerro, J. M., & Lapuerta, V. (2023). Experimental verification and comparison of fuzzy and PID controllers for attitude control of nanosatellites. *Advances in Space Research*, 71, 3613-3630. <https://doi.org/10.1016/j.asr.2022.05.055>
- [6]. Sanyal, S., Barai, R. K., Chattopadhyay, P. K., & Chakraborty, R. (2012). Design of attitude control system of space satellite. *International Journal of Advanced Engineering Technology*, 3(2), 13-16.
- [7]. Narkiewicz, J., Sochacki, M., & Zakrzewski, B. (2020). Generic model of a satellite attitude control system. *International Journal of Aerospace Engineering, Volume 2020*, Article ID 5352019, 1-17. <https://doi.org/10.1155/2020/5352019>
- [8]. Jin, L., & Li, Y. (2022). Model predictive control-based attitude control of under-actuated spacecraft using solar radiation pressure. *Aerospace*, 9, 498, 1-20. <https://doi.org/10.3390/aerospace9090498>
- [9]. Jin, L., & Li, Y. (2022). Model predictive control-based attitude control of under-actuated spacecraft using solar radiation pressure. *Aerospace*, 9, 498, 1-20. <https://doi.org/10.3390/aerospace9090498>
- [10]. Ar-Ramahi, S. K. H. (2009). PID controller design for the satellite attitude control system. *Journal of Engineering*, 15(1), 3312-3320.
- [11]. Ar-Ramahi, S. K. H. (2009). PID controller design for the satellite attitude control system. *Journal of Engineering*, 15(1), 3312-3320.
- [12]. Enejor, E.U., Dahunsi, F. M., Akingbade, K. F., & Nelson, I. O. (2023). Low Earth orbit satellite attitude stabilization using linear quadratic regulator. *European Journal of Electrical Engineering and Computer Science*, 7(3), 17-29. <http://dx.doi.org/10.24018/ejece.2023.7.3.505>
- [13]. Okasha, M. Idres, M., & Ghaffar, A. (2019). Satellite attitude tracking control using Lyapunov control theory. *International Journal of Recent Technology and Engineering*, 7(6S), 253-257.
- [14]. Dass, A. D., Sanusi, H., & Muad, A. M. (2019). Stabilizing roll, pitch and yaw angles for attitude control system (ACS) using direct torque control (DTC). *International Journal of Advanced Trends in Computer Science and Engineering*, 8(1.6), 263-267. <https://doi.org/10.30534/ijatcse/2019/3981.62019>
- [15]. Munusamy, R., Guven, U., & Prakash, O. (2018). Design a nano satellite attitude control system using proportional derivative controller. *International Journal of Research and analytical reviews*, 5(4), 451-459.
- [16]. Si Mohammed, M. A. (2012). Simulation of three axis attitude control using a control momentum gyroscope for small satellites. in *Proceeding of the World Congress on Engineering*, 3, July 4-12, London, U. K.

- [17]. Eze, P. C., & Ezenugu, I. A. (2024). Microsatellite yaw-axis attitude control system using model reference adaptive control based PID controller. *International Journal of Electrical and Computer Engineering Research*, 4(2), 8–16. <https://doi.org/10.53375/ijecer.2024.389>
- [18]. Egwim, E. E., Osuaagwu, I. C., & Emeribe, N. N. (2026). Design of reference model adaptive based discrete-time PID controller for satellite yaw-axis attitude control system. *Asian Journal of Science, Technology, Engineering, and Art*, 4(1), 103-120. <https://doi.org/10.58578/AJSTEA.v4i1.8548>
- [19]. Fritz, M., Shoer, J., Singh, L., Henderson, T., McGee, J., Rose, R., & Ruf, C. (2015). Attitude determination and control system design for the CYGNSS microsatellite. In *Proceeding of IEEE Aerospace Conference, March, 1-12*. <https://www.researchgate.net/publication/276293159>
- [20]. Ajiboye, A. T., Popoola, J. O., Oniyide, O., & Ayinla, S. L. (2020). PID controller for microsatellite yaw-axis attitude control system using ITAE method. *TELKOMNIKA Telecommunication, Computing, Electronics and Control*, 18(2), 1001-1011. <https://doi.org/10.12928/TELKOMNIKA.v18i2.14303>
- [21]. Eze, P. C., Muoghalu, C. N., Uebari, B., & Egbunugha, C. A. (2022). State variable feedback control of data centre temperature. *International Journal of Advanced Networking and Applications*, 14(1), 5250-5257.
- [22]. Nagrath, I. J., & Gopal, M. (2005). *Control systems engineering*. New Age International Publishers, New Delhi.
- [23]. Ekengwu, O. E., Eze, P. C., Asiegbo, C. N., Olisa, S. C., & Udechukwu, C. F. (2022). Satellite dish antenna control for distributed mobile telemedicine nodes. *International Journal of Informatics and Communication Technology*, 11(3), 206-217. DOI: 10.11591/ijict.v11i3.pp206-217
- [24]. Frank, L., Vrabie L. D., & Symos, V. L. (2012). *Optimal Control*. 3rd Edition, John Wiley and Sons, New Jersey, USA.
- [25]. Eze, P. C., Nwadike, S. U., Oyiogu, D. C., & Iroegbu, M. C. (2025). Hybrid PID-LQR controller for dynamic response and stability enhancement of synchronous generator's AVR system. *Asian Journal of Science, Technology, Engineering, and Art*, 3(3), 866-879. <https://doi.org/10.58578/AJSTEA.v3i3.5693>
- [26]. Ekengwu, B. O., Eze, P. C., Muoghalu, C. N., Asiegbo, C. N., & Achebe, P. N. (2024). Design of robust centralized pid optimized LQR controller for temperature control in single-stage refrigeration system. *Indonesian Journal of Electrical Engineering and Informatics*, 12(3), 726-738. <https://doi.org/10.52549/ijeei.v12i3.5629>